International Journal of Remote Sensing and Earth Sciences Vol.13 No. 2 December 2016: 151 – 157

HAZE REMOVAL IN THE VISIBLE BANDS OF LANDSAT 8 OLI OVER SHALLOW WATER AREA

Kustiyo[1,*)], and Anis Kamilah Hayati[2]
[1]Remote Sensing Technology and Data Center, LAPAN
*) e-mail: kustiyo@lapan.go.id

Received: 18 July 2016 ; Revised: 31 August 2016; Approved: 25 November 2016

Abstract Haze is one of radiometric quality parameters in remote sensing imagery. With certain atmospheric correction, haze is possible to be removed. Nevertheless, an efficient method for haze removal is still a challenge. Many methods have been developed to remove or to minimize the haze disruption. While most of the developed methods deal with removing haze over land areas, this paper tried to focus to remove haze from shallow water areas. The method presented in this paper is a simple subtraction algorithm between a band that reflected by water and a band that absorbed by water. This paper used data from Landsat 8 with visible bands as a band that reflected by water while the band that absorbed by water represented by NIR, SWIR-1, and SWIR-2 bands. To validate the method, a reference data which relatively clear of cloud and haze contamination is selected. The pixel numbers from certain points are selected and collected from data scene, results scene and reference scene. Those pixel numbers, then being compared each other to get a correlation number between data scene to reference scene and between result scene and reference scene. The comparison shows that the method using NIR, SWIR-1, and SWIR-2 all significantly improved correlations numbers between result scene with reference scene to higher than 0.9. The comparison also indicates that haze removal result using NIR band had the highest correlation with reference data..

Keywords: *haze removal, shallow water, Landsat 8*

1 INTRODUCTION

Optical sensors in remote sensing satellite detect solar radiation from particular objects at a certain location and time. Those radiation numbers then converted to reflectance number which is a representation of those particular objects. A reflectance number that acquired by sensor could be different from the actual (in situ) reflectance number caused by an atmospheric condition which affect the quality of remote sensing imagery.

Generally, there are three aspects that affect the quality of remote sensing imagery; radiometric quality, geometric quality, and atmospheric quality (Shahrokhy, 2004). The atmospheric effects that cause image contamination are cloud and haze. Cloud cover blocks almost all reflected radiation from the surface so the only information loss recovery method that available is substitution using multi-temporal imagery (Lu, 2007). Haze partially obscures the ground, therefore using atmospheric correction techniques, theoretically, haze is possible to be removed (Liu *et al.*, 2011).

The quality of remote sensing imagery has been very important since the quality of imagery corresponds with accuracy and reliability of extracting information (Xia and Chen, 2015). The atmospheric correction of satellite images is an important step to improve the data analysis. Performing atmospheric correction could ease comparison between multi-temporal, improved the results of change detection and classification algorithms, gain possibilities to compare ground reflectance data of different sensors with similar spectral bands, enable comparison between ground reflectance data retrieved from satellite imagery and ground measurements which providing an opportunity to verify the results, and atmospheric correction based on simultaneous atmospheric and ground reflectance measurements allows the monitoring of the radiometric sensitivity of space-borne sensors (inflight calibration) (Richter 1996a).

An efficient method for haze removal is still a challenge. (Caselles and García 1989) used multi-temporal data to complete information that covered by haze. (Chavez, 1988) developed simple dark-object subtraction method and improved by (Makarau *et al.*, 2014). (He, Sun, and Tang 2011) proposed dark channel prior calculation to estimate haze thickness for RGB imagery. (Richter 1996b) developed a haze removal method to transition between haze and non-haze regions. (Liu *et al.*, 2011) presented background suppressed haze thickness index technique to indicate haze thickness. While all the methods described above deal with land areas, this paper tries to focus to remove haze at water areas.

Since the climate in Indonesia is tropical, the clear scenes of remote sensing imageries are hard to be collected. That is why radiometric correction needs to be done to increase the availability of clear data, especially for Landsat 8 data.

This paper's goal is to remove or minimize haze disruption over shallow water areas. The radiometric correction present in this paper could be used for further and better coral reefs analysis or classification.

A simple method using a subtraction algorithm is presented in this paper. The method elaborates a methodology developed by (Ji, 2007) which used the NIR band from Landsat-5 and Landsat-7 imageries to estimate the spatial distribution of haze intensity. Differ from (Ji, 2007) this paper used NIR, SWIR-1, and SWIR-2 bands from Landsat 8 imagery. The results from each band then compared with a reference scene to test the accuracy. Reference scene that have been selected is the scene from the same path and row with minimum cloud and haze interference.

2 MATERIALS AND METHODOLOGY

2.1 Data and Location

Data used in this experiment are Landsat 8 imageries from path 114 row 064 which cover part of the South Sulawesi area. Landsat 8 Operational Land Imager (OLI) consists of 9 spectral bands with a spatial resolution of 30 meters for Bands 1 to 7 and 9 (USGS, 2016). The bands used in this paper are visible, NIR, SWIR-1, and SWIR-2 bands. Multi temporal data are used for comparison, imagery with haze area is used as a data model and imagery with relatively clear from haze is used to validate. Data acquired in August, 9th 2016 is used as data model while data acquired in July, 24th 2016 is used as evaluators. Pre-processing data including top of atmosphere (TOA) are conducted

2.2 Haze Removal Method

Haze can be interpreted as spatially varying, semitransparent cloud and aerosol layers (Zhang *et al.*, 2002). As artifacts, haze effect sensor from accurately detecting radiance from ground object. Due to multiple scattering of incoming and outgoing radiations through the haze relative to the ground, the signal recorded from each ground pixel cannot be considered as the arithmetic sum of the radiance contributed by the haze and the radiance contributed by the ground pixel (Lavreau 1991).

To simplify the complex arithmetic, this paper employs assumptions (Figure 2-1). The basic idea is, for bands that reflected by water (visible bands), a radiance total that detected by sensor is a sum from radiance scattered by water and radiance scattered by haze (Equation 2-1). While for bands that absorbed by water (NIR, SWIR-1, and SWIR-2 bands), a radiance total that detected by the sensor is equal to radiance scattered by haze (Equation 2-2). This basic idea is developed by (Ji, 2007) which used visible and NIR bands from Landsat-5 and Landsat-7. This paper modified and examined the previous paper by using bands from Landsat 8 and adding SWIR-1 and SWIR-2 bands to see the correlation.

$$Rad_{\lambda i}{}^{ho} \approx Rad_{\lambda i}{}^{tot} - Rad_{\lambda i}{}^{haze} \qquad (2\text{-}1)$$

$$Rad_{\lambda j}{}^{tot} \approx Rad_{\lambda j}{}^{haze} \qquad (2\text{-}2)$$

Where $Rad_{\lambda i}{}^{ho}$ represent radiance reflected by water without haze contamination. $Rad_{\lambda i}{}^{tot}$ represent total radiance that received at the sensor. $Rad_{\lambda i}{}^{haze}$ represent radiance reflected by haze as contamination. i represent band that reflected by water (visible bands).

Where $Rad_{\lambda j}{}^{tot}$ represent total radiance received at the sensor. $Rad_{\lambda j}{}^{haze}$ represent radiance that reflected by haze. j represent band that absorbed by water (visible bands).

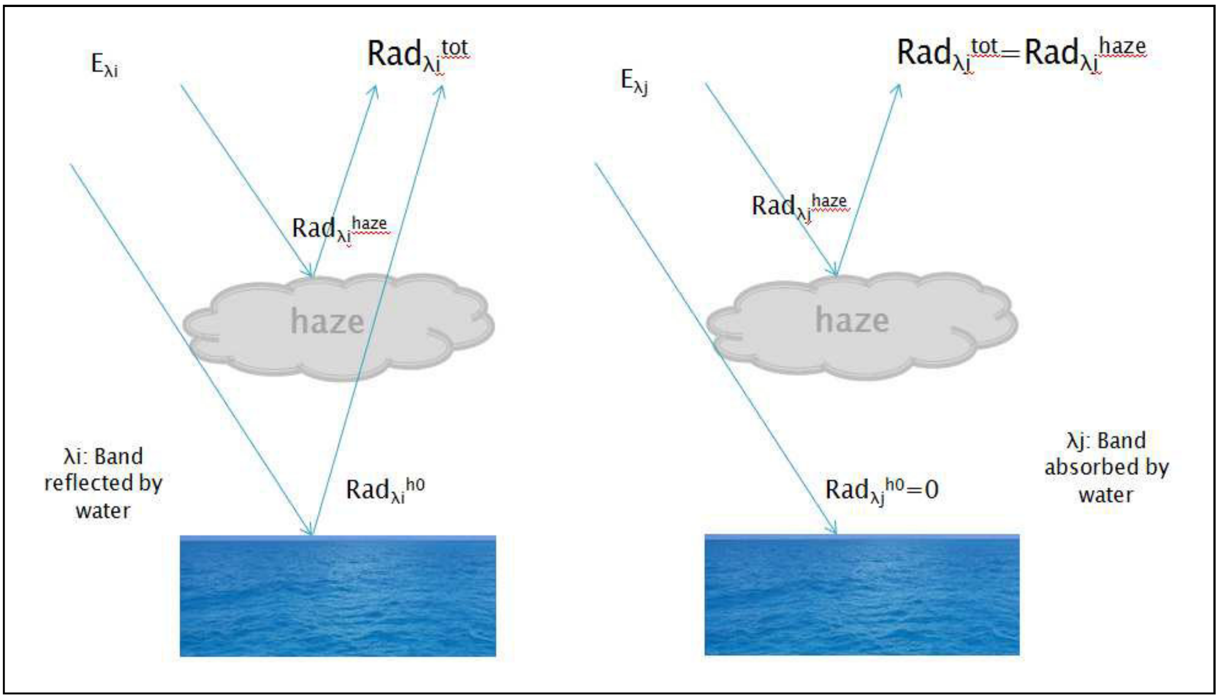

Figure 2-1: Basic Idea of Radiance Detected by Sensor from Hazy Area

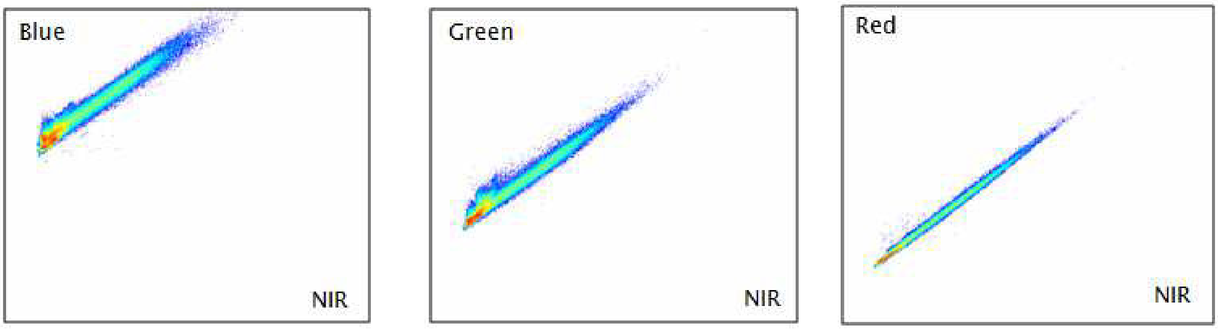

Figure 2-2: Correlation Between Visible Bands and NIR Band

In some manners, band reflected by water is correlated with band absorbed by water (Figure 2-2). In that case, linear correlation could be determined (Equation 2-3), and Equation 2-1 could be rewritten as Equation 2-4.

$$Rad_{\lambda i}{}^{ho} \approx \alpha_{ij} * Rad_{\lambda j}{}^{haze} + \beta_{ij} \qquad (2\text{-}3)$$

Where α and β shows regression coefficients.

$$Rad_{\lambda i}{}^{ho} \approx Rad_{\lambda i}{}^{tot} - \left(\alpha_{ij} * Rad_{\lambda j}{}^{haze} + \beta_{ij}\right). \qquad (2\text{-}4)$$

2.3 Validation Method

To validate the result, multitemporal scene was used. The selected scene is a scene which has minimum cloud and haze contamination among another scene from the same path and row. This scene is not fully free from cloud and haze, therefore some points that visually clear from cloud and haze are determined. Those points, compared to points from results scene exactly in the same positions, are conducted as material to establish validation.

Pixel numbers for each point are collected from the scene before haze removal conducted; results scene from each NIR, SWIR-1, and SWIR-2 bands; and also from reference scene. Those pixels from every scene then compared one to another and the produced correlation number. The highest correlation number indicates the best result.

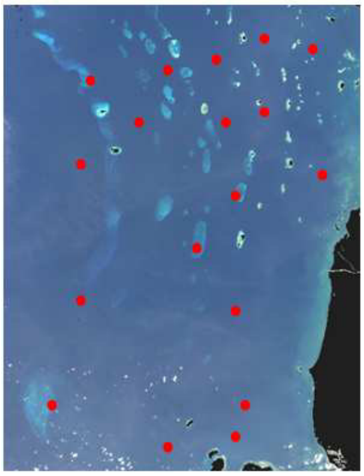

Figure 2-3: Points Determined from Reference Scene

3 RESULTS AND DISCUSSION

Figure 3-1 shows the data from haze removal result using the method described before. As seen from the picture, each haze removal result using NIR, SWIR-1, and SWIR-2 band indicates transformation. Hazy area evidently on top-right corner in Figure 3-1 (a) is reduced and seemed like a non-hazy area in Figure 3-1 (b, c, d).

To validate the results, reference data are used. 100 points from reference data that believed as clear area are selected. The pixel number of those points, then compared to pixel number collected from result scenes. At the exact positions as points in reference data. The pixel number correlation between scene before haze removal, NIR band result scene, and reference scene are shown in Figure 3-2.

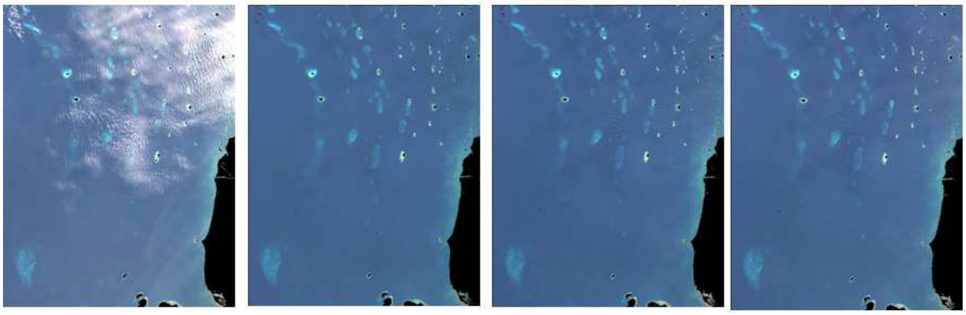

(a) (b) (c) (d)

Figure 3-1: Haze Removal Result. (a) RGB Natural Color Imagery (b) Haze Removal Using NIR Band (c) Haze Removal Using SWIR-1 Band (d) Haze Removal Using SWIR-2 Band

Correlation is used to measure the degree of data similarity between result scene and reference scene. Correlation numbered 1 show that the result scene is similar to reference scene. Thus the better method is presented with the closest its correlation number to 1.

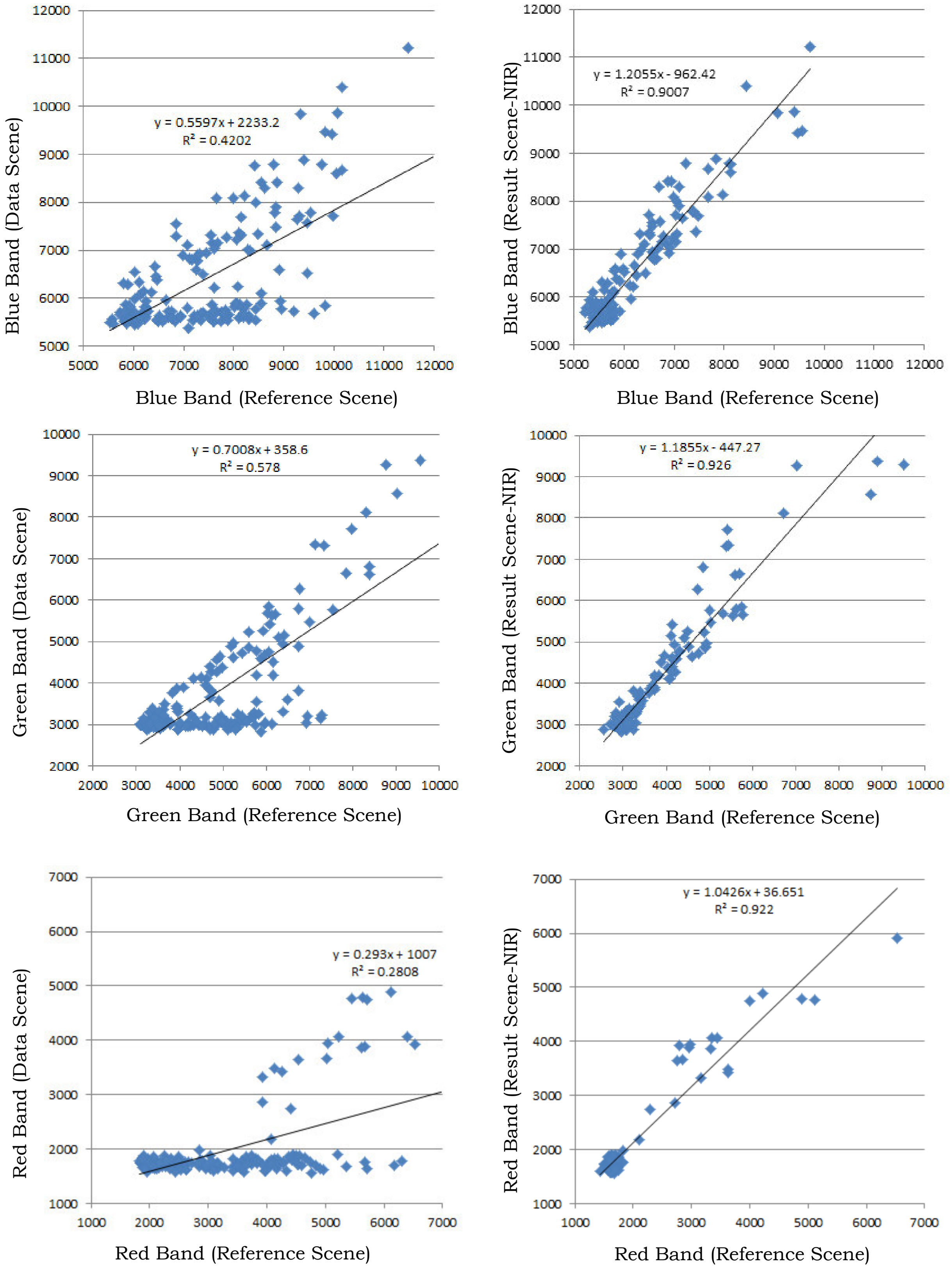

Figure 3-2: Pixel Number Correlation Between Reference Scene with Data Scene and NIR-Result Scene

The pixel Number correlation between reference data and results from each band are displayed in Table 3-1. Haze removal results using NIR, SWIR-1, and SWIR-2 all increased correlation number from the data before haze removal is applied. At the Table 1 showed, haze removal result using NIR band had the highest correlation with reference data. Not too far behind, both SWIR-1 and SWIR-2 also highly correlated with reference data.

For RGB band, the highest correlation reached by the Green Band followed by Red and Blue Band. The resulting scenes (using NIR, SWIR-1, and SWIR-2) and reference scene have Green Band as the most similar band to each other. Using NIR band, the similarity of Green Band between result scene and reference scene reaches the highest which is 0.962. Furthermore the lowest similarity is 0.916 which is the similarity for Blue Band between reference scene and result scene using SWIR-1.

Compared to the data before haze removal is applied, all result scenes have better correlation with referenced scene. The correlation between the referenced scene and result scenes are increased for average 1.5 times than before haze removal is applied. This shows that the method enhance radiometric quality significantly.

Table 3-1: Correlation Between Reference Data and Results

	Red Band	Green Band	Blue Band	Average
Data Before Haze Removal	0.530	0.760	0.648	0.646
Result Using NIR Band	0.960	0.962	0.949	0.957
Result Using SWIR-1 Band	0.926	0.952	0.916	0.931
Result Using SWIR-2 Band	0.938	0.956	0.927	0.940

Although theoretically SWIR-2 band is the band that absorbed by water the most, the results show that haze removal result using NIR band has the highest correlation with reference data. It is possibly because the NIR band also has the highest correlation with the visible band in term of cloud detection rather than SWIR-1 or SWIR-2 bands. These results conformable previous paper presented by (Ji, 2007) which conclude that proposed algorithm using NIR band can be implemented to significantly improve the visual interpretability of images acquired under hazy conditions.

4 CONCLUSION

Methodology for haze removal from visible bands of Landsat 8 over the shallow water area is presented in this paper. NIR, SWIR-1, and SWIR-2 bands can be used to be implemented in the method. Haze removal result using NIR, SWIR-1, and SWIR-2 all give visually good improvement, as a hazy area in imagery reduced greatly. Although the image result using NIR, SWIR-1, and SWIR-2 bands, all highly correlated with reference data, image result using NIR band has the highest correlation number with reference data.

Therefore, since every visible band in the result image highly correlated with reference data (higher that 0.9), it can be said that the method works well using every band (NIR, SWIR-1, and SWIR-2). Nevertheless, because the method based on the assumptions of single scattering in the radiometric interaction process, further validation is required and quantitative analysis should be done with caution.

ACKNOWLEDGEMENT

The Author would like to thank to Pustekdata LAPAN for funding and providing data and infrastructures needed for this research. We also like to thank to everyone that's involved in the making of this paper: Landsat 8 acquisition team that have granted the access to Landsat 8 data, Dr. Jonson Lumban Gaol as Focus Group Discussion supervisor, all of Focus Group Discussion team, and all of our colleagues in Pustekdata LAPAN.

REFERENCES

Caselles V., García MJL, (1989), An Alternative Simple Approach to Estimate Atmospheric Correction in Multitemporal Studies. International Journal of Remote Sensing 10(6): 1127–34.

Chavez PS, (1988), An Improved Dark-Object Subtraction Technique for Atmospheric Scattering Correction of Multispectral Data. Remote Sensing of Environment 24(3): 459–79.

He K., Sun J., Tang X., (2011), Single Image Haze Removal Using Dark Channel Prior. IEEE Transactions on Pattern Analysis and Machine Intelligence 33(12): 2341–53.

Ji CY, (2007), Haze Reduction from The Visible Bands of LANDSAT TM and ETM+ Images Over A Shallow Water Reef Environment. Remote Sensing of Environment 112(4): 1773–1783. doi: 10.1016/j.rse.2007. 09.006.

Lavreau J., (1991), De-hazing Landsat Thematic Mapper images. Photogrammetric Engineering & Remote Sensing 57(10): 1297−1302.

Liu C., Hu J., Lin Y., Wu S., Huang W., (2011), Haze Detection, Perfection and Removal for High Spatial Resolution Satellite Imagery. International Journal of Remote Sensing 32 (23): 8685–8697.

Makarau A., Richter R., Muller R., Reinartz P., (2014), Haze Detection and Removal in Remotely Sensed Multispectral Imagery. IEEE Transactions on Geoscience and Remote Sensing 52(9): 5895–5905. doi: 10. 1109/TGRS.2013.2293662.

Richter R., (1996a), A Spatially Adaptive Fast Atmospheric Correction Algorithm. International Journal of Remote Sensing 17 (6): 1201–14.

Richter R., (1996b), Atmospheric Correction of Satellite Data with Haze Removal Including a Haze/clear Transition Region. Computers and Geosciences 22 (6): 675–81.

Shahrokhy SM, (2004), Visual and Statistical Quality Assessment and Improvement of Remotely Sensed Images. ISPRS Proceedings XXXV (950).

United States Geological Survey, (2016), LANDSAT 8 (L8) DATA USERS HANDBOOK. Retrieved from https://landsat.usgs.gov/documents/Landsat8DataUsersHandbook.pdf on October 28, 2016.

Xia Y., Chen Z., (2015), Quality Assessment for Remote Sensing Images: Approaches and Applications. IEEE International Conference on Systems, Man, and Cybernetics. doi: 10.1109/SMC.2015.186.

Zhang Y., Guindon B., Cihlar J., (2002), An Image Transform to Characterize and Compensate for Spatial Variations in Thin Cloud Contamination of Landsat Images. Remote Sensing of Environment 82 (2-3): 173–87.